Mechanical Characterization of Jammable Granular Systems

By

Shaymus William Hudson

Submitted to the Department of Materials Science and Engineering in partial fulfillment of the requirements for the degree of

Bachelor of Science

at the

MASSACHUSETTS INSTITUTE OF TECHNOLOGY

May 2012

Signature of Author…….....
Department of Materials Science and Engineering
May 4, 2012

Certified by…….....
Neri Oxman
Sony Corporation Career Development Professor of Media Arts and Sciences
Thesis Supervisor

Read by…….....
Lorna J. Gibson
Matoula S. Salapatas Professor of Materials Science and Engineering
Thesis Reader

Accepted by...…….....
Jeffrey C. Grossman
Carl Richard Soderberg Associate Professor of Power Engineering
Chair, Undergraduate Committee

Mechanical Characterization of Jammable Granular Systems

By

Shaymus William Hudson

Submitted to the Department of Materials Science Engineering
on May 4, 2012
in partial fulfillment of the requirements for the
degree of
Bachelor of Science

Abstract

The mode by which a granular material can transition between fluid-like and solid-like states has been often referred to as jamming. The use of this property (via vacuum pressure) for engineering applications has only recently been explored. Several possible applications are presented. However, thorough characterization of mechanical properties and material selection for jammed systems has not been reported. Glass beads of differing size distributions, silica blasting media, sand, and ground coffee were tested under different vacuum pressures in a procedure similar to an unconsolidated-undrained triaxial compression test for soils. Coffee was found to have the highest strength to weight ratio. Literature predictions of the trend between applied pressure and effective Young's modulus was also investigated.

Thesis Supervisor: Neri Oxman

Title: Sony Corporation Career Development Professor of Media Arts and Sciences

Table of Contents

List of Figures

List of Tables

Acknowledgements

I am thankful for the opportunity to perform my undergraduate thesis research under Professor Neri Oxman, as it allowed me to pursue a thesis topic that was engaging and very interesting. The entire project would not have been possible, however, without the help of several graduate students. First, I thank Steven Keating of the Mediated Matter Group who helped direct my initial research and gave me advice on my work during the summer and throughout the school year, even as he was writing his own thesis and teaching. Second, I thank Nadia Cheng of the Hatsopolous Microfluids Laboratory for access to her microscope and granular media. I also thank Professor Lorna Gibson for her lab space and Instron for initial testing as well as Dr. John Germaine from the Civil Engineering Department for advice on testing methods.

I am also thankful for the support of my family throughout the years especially my parents and sisters, Lynsie and Shelby. I would also like to thank my friends from Course III, the Concourse Program, East Campus, and all of those whom I had the honor of meeting during my time at the Institute, for making the past four years the experience of a lifetime.

Chapter 1: Introduction

1.1 Jamming Theory

Granular materials, such as sand or table salt, can flow when they are shaken or poured through a hopper but can clog up when the shaking intensity or pouring rate is decreased. Similarly, foams and emulsions (dense colloidal suspensions of deformable gas bubbles or liquid droplets) can flow when they are sheared but are soft amorphous solids when the shear stress is lowered below the yield stress. This mechanism by which a granular material can reversibly transition between fluid-like and solid-like states has been often referred to as jamming. Jamming arrangements can serve as useful models for systems like glasses, liquids, and materials with characteristic internal structure. A simple example of jamming can be seen in figure 1, where the particles in red are placed in a jammed state, preventing flow through the hopper. The red particles structurally act as an arch, which forces the ensemble to act as a solid.

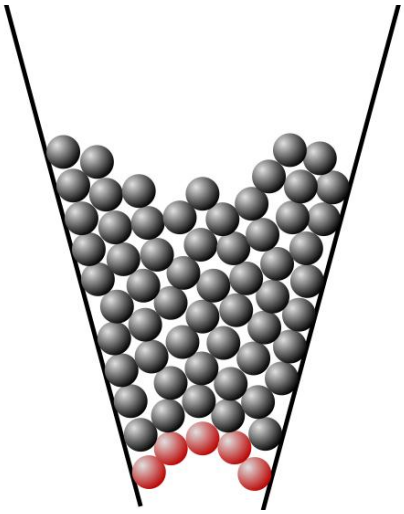

Figure 1 – An example of jamming in a 2D hopper. The particles in red are jammed such that the particle ensemble behaves like a solid until there is enough energy to unjam it.

The definition of jammed states, developed and refined by Salvatore Torquato at Princeton University, includes the notions of local, collective, and strictly jammed configurations – configurations which are based on the number of grain contacts and degrees of freedom of each grain. Given a given a system of N spheres, a particle is said to be individually jammed if it cannot be translated while holding fixed all the positions of all other N-1 particles in the system. The ensemble can then be in three possible jamming configurations. The system is in a:

(1) locally jammed configuration if the system boundaries are non-deformable and each of the N particles is individually jammed,

(2) collectively jammed if the system boundaries are non-deformable and it is a locally jammed configuration in which there can be no collective motion of any contacting subset particles that leads to unjamming,

(3) strictly jammed if it is collective jammed and the configuration remains fixed under infinitesimal virtual global deformations of the boundaries. No global boundary-shape changes accompanied by collective particle motions can exist.[1]

Using these definitions, theoretical models of the jamming transition have developed into a so-called jamming "phase-diagram" (figure 2). Since a granular material's structure is similar to that of an amorphous solid, yield stress and dynamical transition temperature are drawn as curves. While the shape of the surface will vary

from system to system, the space (with respect to temperature, applied stress, and density) helps identify important design parameters.[2,3]

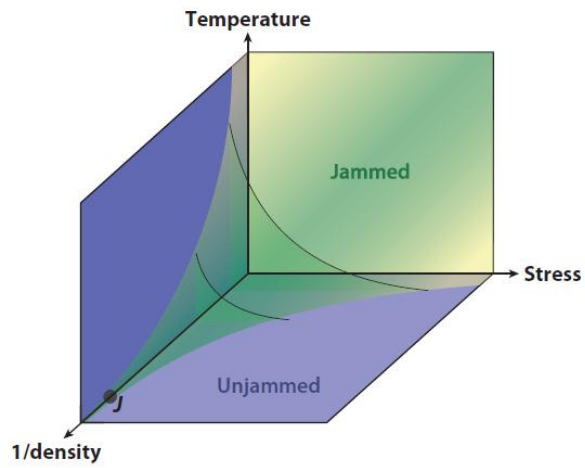

Figure 2 – Pseudo phase diagram exhibiting parameters for the jamming transition. Point J identifies the point of jamming for frictionless, perfect spheres.[2]

From figure 2, it can be seen that jammed states are not only created by the configuration of particles, but also by the physical boundaries of the system. In a system of small particles, the transition to jam also occurs when the applied stress or density is sufficiently large. At low packing fractions, particles are free to diffuse into different configurations. As the packing fraction increases, the space available for motion decreases and the system becomes a disordered solid with a yield stress.[4]

Disciplines within civil engineering, such as soil mechanics, often treat granular media as a continuum to analyze bulk mechanical properties. In uniaxial experiments conducted by Sidney Nagel at the University of Chicago, the distribution of stresses in a jammed ensemble varies upon the number of contacts within the

system.[5] For example, media compressed in a cylinder exhibits a change in force distribution with the cylinder radius. This is due to particles in the bulk having a higher contact number than those on the surface. In addition to than the contact number, factors that contribute to the mechanical performance of jammed media include the mechanical characteristics of the grain material and morphologies present in the ensemble. For example non-deformable perfect spheres will have different packing characteristics than rough, jagged, deformable particles.

It has been shown that differing particle morphologies direct how well granular media can flow and compact.[6] Also, as seen in Figure 3, computer models have indicated that for frictional spheres, ensemble properties such as bulk and elastic modulus tend to increase with internal pressure and coordination number.[7] It has been shown for jammed spheres, the bulk effective elastic modulus varies as a power law with increasing packing fraction.[8]

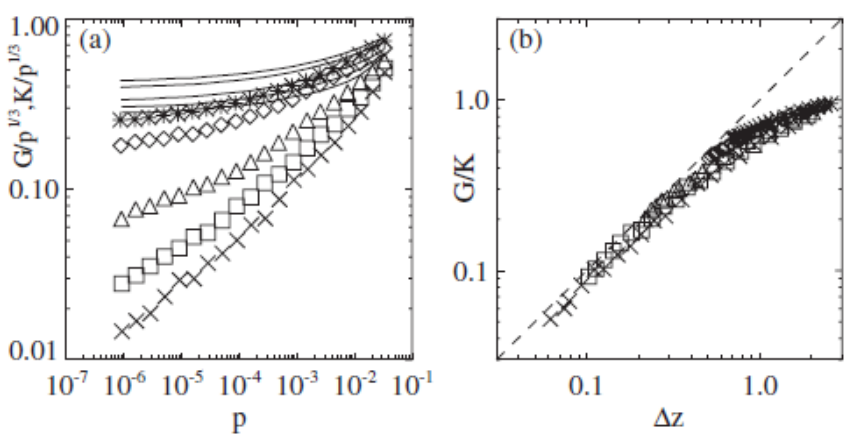

Figure 3 – Trends between a) internal stress between particles p (in pascals) and bulk and elastic modulus G and K, respectively. Lines represent K and points represent G for different frictional coefficients. The curves go up the graph for decreasing friction coefficient, b) coordination number Δz and modulus ratio.[7]

1.2 Current Art and Possible Applications

Only recently have researchers explored the use of granular materials for engineering purposes. For example, a team from the University of Chicago, Cornell University, and iRobot has developed a universal gripper that can passively conform to and grasp a wide range of objects.[9] Other applications include variable force feedback in haptic interfaces, morphable robots, and a method for casting prosthetic limbs in developing countries.[10,11,12,13] All of these potential applications take advantage of atmospheric pressure to induce jamming via a vacuum pump. The Mediated Matter group at the MIT Media Lab also demonstrated potential applications of the jamming transition for morphable rigid forms, some of which are demonstrated in Figure 4.

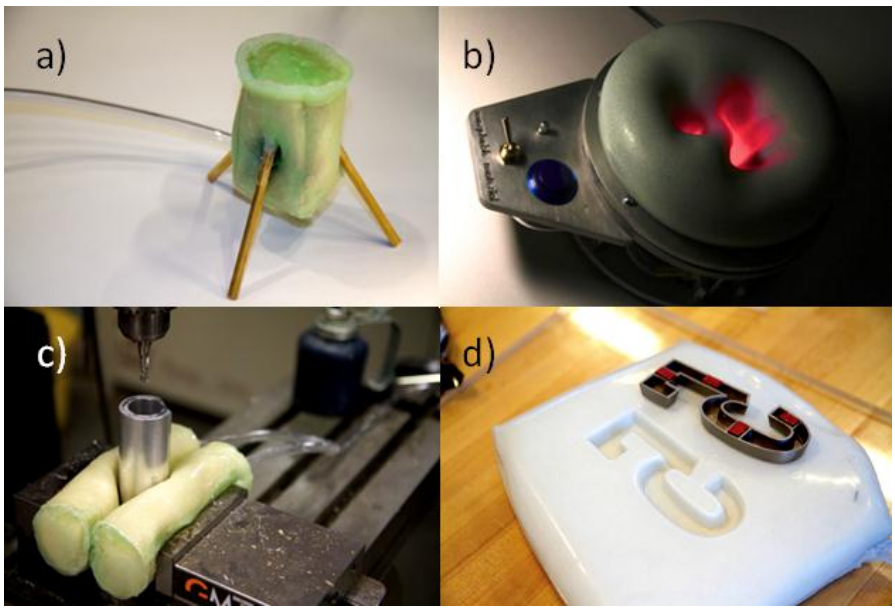

Figure 4 – Possible applications of jamming; a) universal joint, b) aesthetics and art, c) vice grip soft jaws, d) low volume casting

New innovations with jamming include structural applications such as a universal joint (Figure 4a), which would allow for different structural geometries of the bulk material as well as translational configurations of each of the pin joints or arms. In addition, a morphable chair using this principle can be arranged into any configuration and jammed to create a rigid form capable of supporting a person. A flexible vice (Figure 4c) using jamming has also been successfully demonstrated and could eliminate the need for machining soft jaws.

Other avenues for jamming include low temperature casting (Figure 4d). A vacuum casting system using granular media can rapidly create a reusable custom mold without the need for external heat and waste materials. After parts are cast, they can be easily removed by applying pressure inside the granular system to push to part out. In our prototypes, cast parts have been reproduced with a number of materials including thermoset plastics, chocolate, pewter, and bismuth.[14]

1.3 Problem Statement

The goal of this thesis was two-fold. I endeavored to further the use and understanding of jamming by beginning to determine the necessary mechanical properties for engineering applications. I sought to determine the effective Young's elastic moduli, yield stresses, and strength to weight ratio of various granular mixtures for aid in materials selection. Also, I wanted to investigate the calculated power law trend between internal stress (in this case simulated by vacuum pressure) and effective Young's modulus.

Chapter 2: Methods and Materials

2.1 Considerations for Testing

As discussed previously, granular media can be treated as a continuum for mechanical testing. Although there are currently no ASTM (American Society for Testing and Materials) test methods for granular media under vacuum, soil testing methods used in civil engineering offer guidance. The methods used were based upon ASTM D2850, the unconsolidated-undrained triaxial compression test.[15] As seen in Figure 5, a cylindrical soil sample contained in a thin, flexible membrane (2:1 height to diameter ratio) is placed under compression in a chamber filled with fluid, such as oil or water. The fluid is then pressurized to place the sample in a triaxial loading condition. Load and displacement data gathered from the experiment can be used to calculate a yield envelope for the sample. The standards of this method were acknowledged in data collection.

To analyze size effects, glass beads were the material of choice since their geometries, size distributions, and coefficients of friction were easily controllable. Play sand, fine blasting grade silica, and coffee grinds were also selected for their variable morphologies as well as their use in current commercial applications and prototypes. A summary of the materials tested are listed in Table 1.

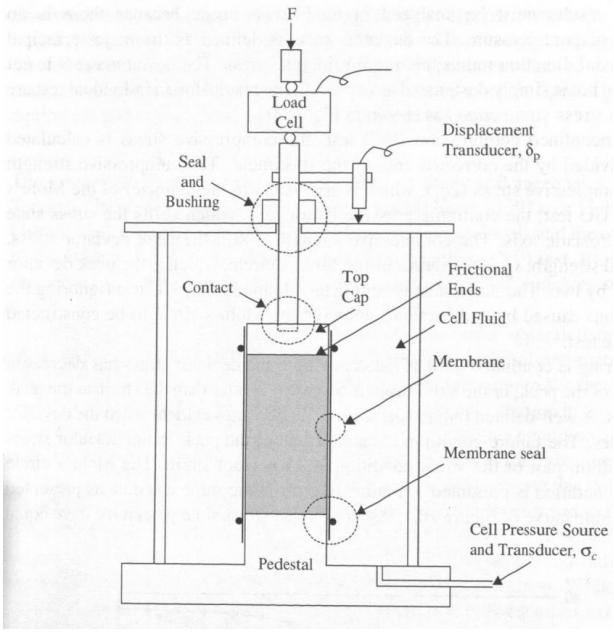

Figure 5 – Schematic of an unconsolidated-undrained triaxial compression test.[15]

Material	Supplier
300-425 µm Silica Beads	MoSci Corporation (North Rolla, MO.)
800-1200 µm Silica Beads	MoSci Corporation (North Rolla, MO.)
1500-2000 µm Silica Beads	MoSci Corporation (North Rolla, MO.)
2000-2500 µm Silica Beads	MoSci Corporation (North Rolla, MO.)
Medium-Fine Silica Blasting Media (149-88 µm)	Kramer Industries (Piscataway, NJ.)
Play Sand	Quickcrete Products Corporation (Norco, CA.)
Ground Coffee	Shopper's Value (Shaw's Supermarket Generic Brand)

Table 1 – Granular materials tested and their respective suppliers

2.2 Media Size Measurement

To observe the geometries and verify sizes of the particles, the granular media were observed under a Nikon (Tokyo, Japan) Eclipse TE2000-S optical microscope with a Matrix Vision (Paris, France) BlueFOX digital camera. All media was observed under a 2x lens. Pictures were taken and manipulated with Streampix III software. Due to the small aperture size on the microscope, 1500-2000 µm and 2000-2500 µm beads were measured using a Mitutoyo (Kawasaki, Japan) 293-344 digimatic micrometer with a 0.001 mm resolution.

2.3 Sample Preparation

To determine mechanical properties, the experiment was set up similarly to ASTM D2850. A cylinder of granular material, contained in a thin, flexible membrane with metal endcaps was connected to a vacuum pump to keep shape and vary the level of pressure on the jammed media. The sample then underwent uniaxial compression to determine a stress-strain curve.

To prepare samples for compression testing, two 6061 aluminum end caps were machined (Figure 6). The bottom cap was drilled with a 3/8 in. and 1/8 in. bit for air to flow out. The flat-faced hole was then covered with a 1 in. by 1 in. square of canvas for filtration and adhered with Silpoxy™ silicone adhesive to provide an air tight seal.

To help the sample maintain its shape, Trojan™ unlubricated latex condoms were used as the membranes described in ASTM D2850. To force the condom to be a cylindrical shell, two attachments were 3D printed out of ABS on a Dimension BST 1200es printer (Figure 7). Perforated holes on the sides of the attachments allowed for the condom to form into a cylinder in vacuum. To prevent the perforations from appearing on the sample surface, the holes were covered with filter paper.

As vacuum pulled on the outside of the condom, granular material was poured into the fixed volume using a funnel to prevent close packing. The particles were then capped off with the aluminum ends. Vacuum was then pulled on the inside of the condom and the granular media through the filtered endcap, after which the attachments were removed (Figure 8 and 9).

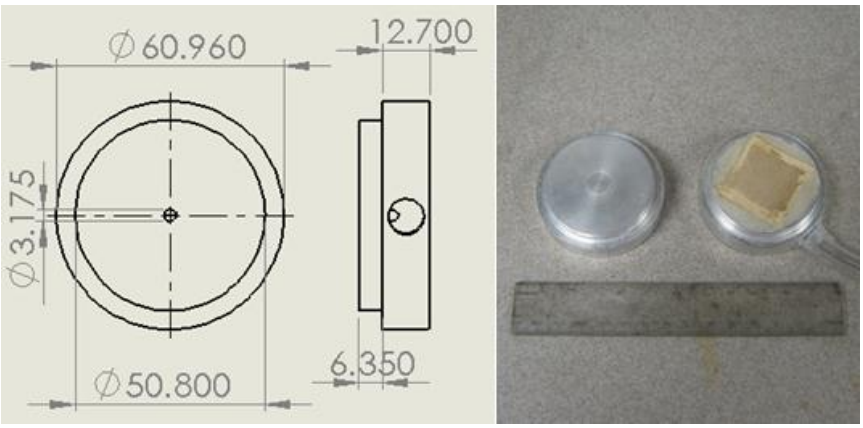

Figure 6 – (Left) Schematic drawing of aluminum endcap with units in mm; (Right) Endcaps after service with adhered filter.

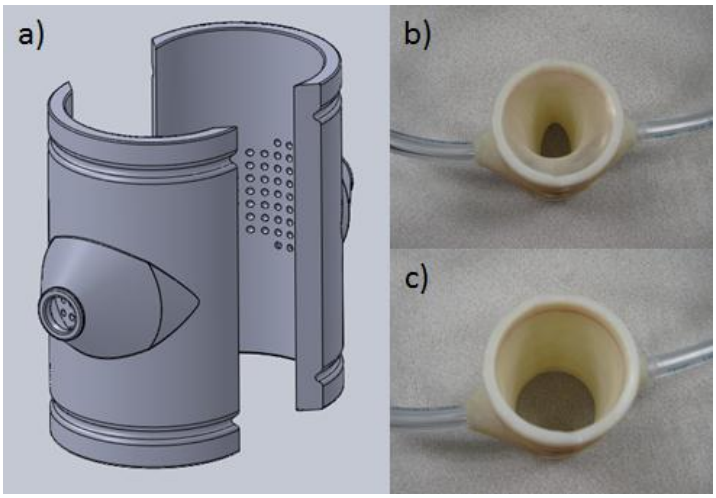

Figure 7 – a) 3D rendering of ABS attachments; b) condom/attachment under no vacuum; c) under vacuum.

2.4 Mechanical Testing Procedure

Prepared specimens were tested in an Instron 4206 mechanical tester using reversible 150 kN load cell which acted as a platen (Figure 9). To control sample vacuum pressure, a FJC vacuum pump with brass fittings was used. Pressure was regulated with a brass ball valve and vacuum gauge (accurate to ±1 MPa). During compression, the machine operated at a strain rate of 2 mm/min and ended at 15 mm platen displacement or until the force-displacement curve sufficiently leveled out. Raw data was gathered and analyzed using Instron Bluehill 2 software with a sampling rate of 100 data points per minute.

Samples were compressed at vacuum pressures of 100, 75, 50, and 25 kPa. For each size of glass beads, three tests were conducted at each pressure to account for the

variability of loose packing. Using the Bluehill software, effective Young's modulus and yield strength were calculated using a least squares algorithm (see appendices). After testing, the granular material was weighed to calculate strength to weight ratios.

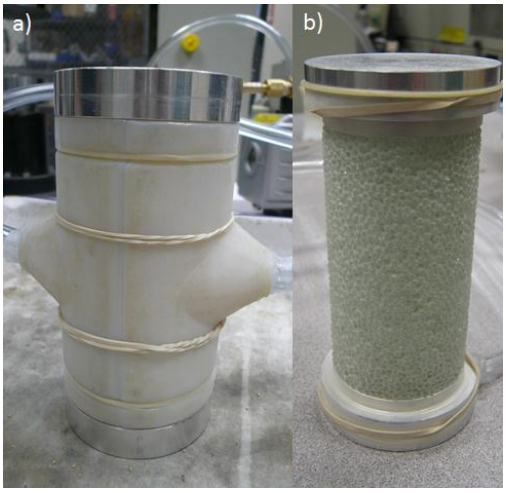

Figure 8 – a) filled sample with ABS attachment; b) fully prepared sample

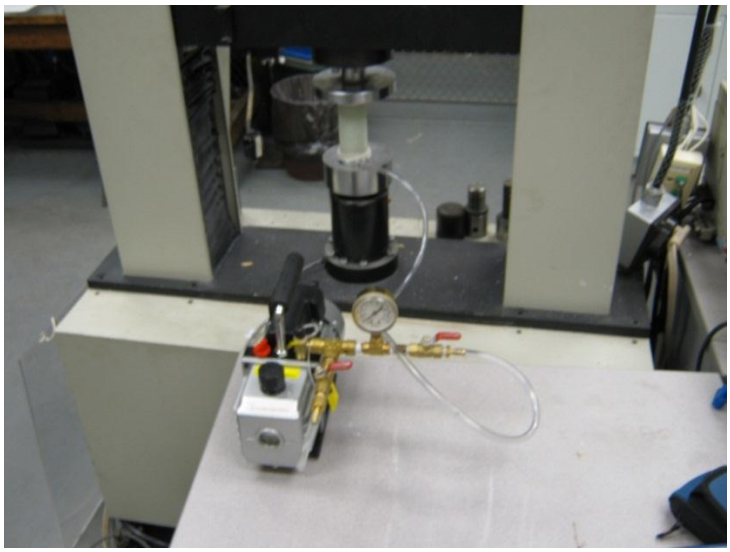

Figure 9 – Experimental setup for testing.

Chapter 3: Results

3.1 Glass Beads

The manufacturer's nominal sizes and shapes of the glass beads were verified from micrographs (Figure 10). Using a sample of twenty beads of each size range, the measured average size fell within reported ranges (Table 2).

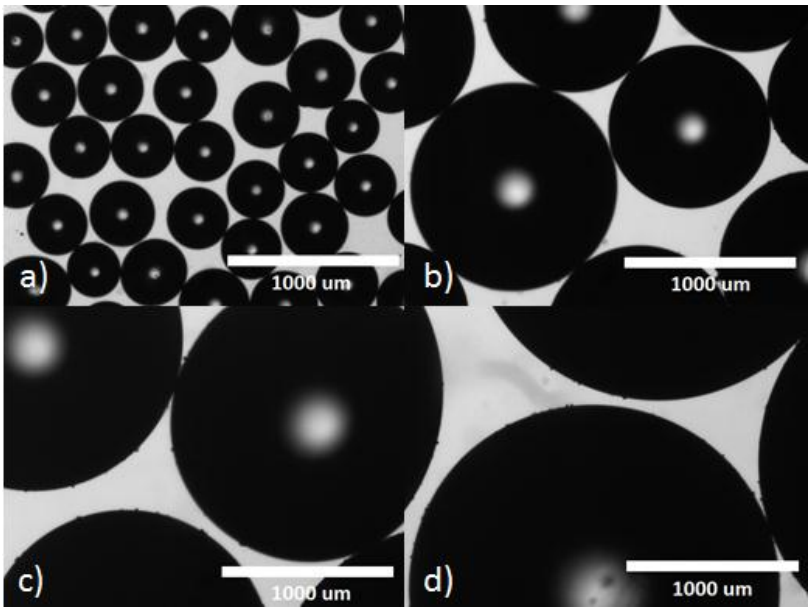

Figure 10 – Micrographs of glass beads of sizes a) 300-425 um, b) 800-1200 um, c) 1500-2000 um, and d) 2000-2500 um

Manufacturer's Nominal Size (µm)	Measured Size (µm)
300-425	349 ± 22
800-1200	1071 ± 112
1500-2000	1775 ± 201
2000-2500	2239 ± 149

Table 2 – Reported and measured sizes of glass beads

For compression tests, both yield stress and Young's modulus are well described by a linear dependence on applied pressure except for the modulus of the 2000-2500 µm beads (Figure 11 and 12). Yield stress also appears to have a linear dependence with bead size (Figure 13). It does not appear to be the case with Young's modulus (Figure 14).

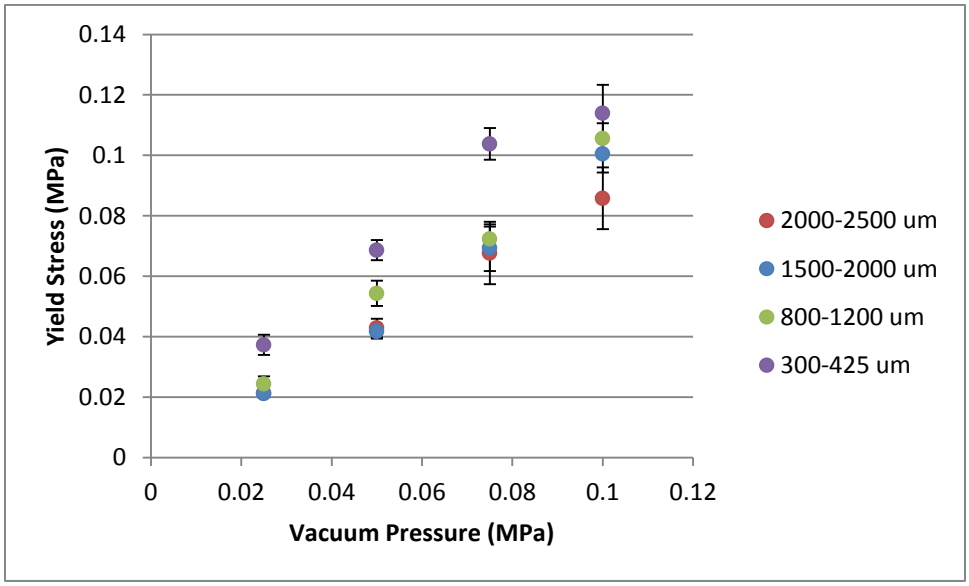

Figure 11 – Plot of ensemble yield stress with respect to vacuum pressure for all glass bead sizes.

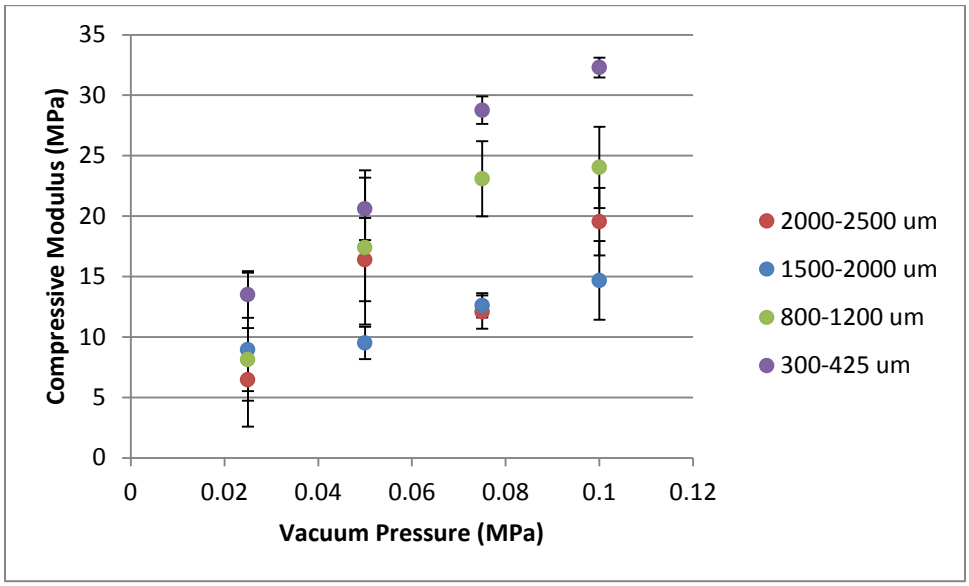

Figure 12 – Plot of effective Young's modulus of glass beads with respect to vacuum pressure.

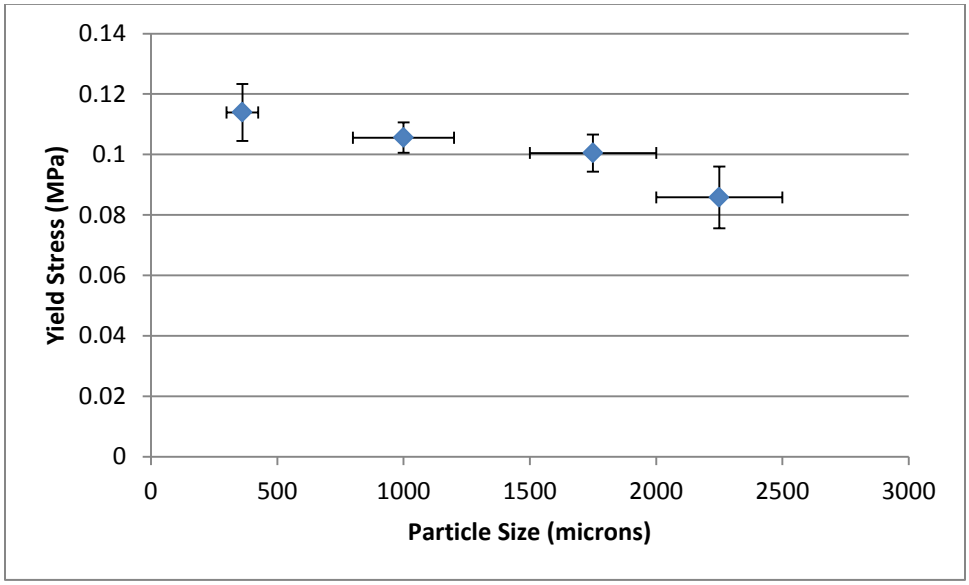

Figure 13 – Plot of glass bead size versus yield stress at maximum vacuum pressure (100 kPa).

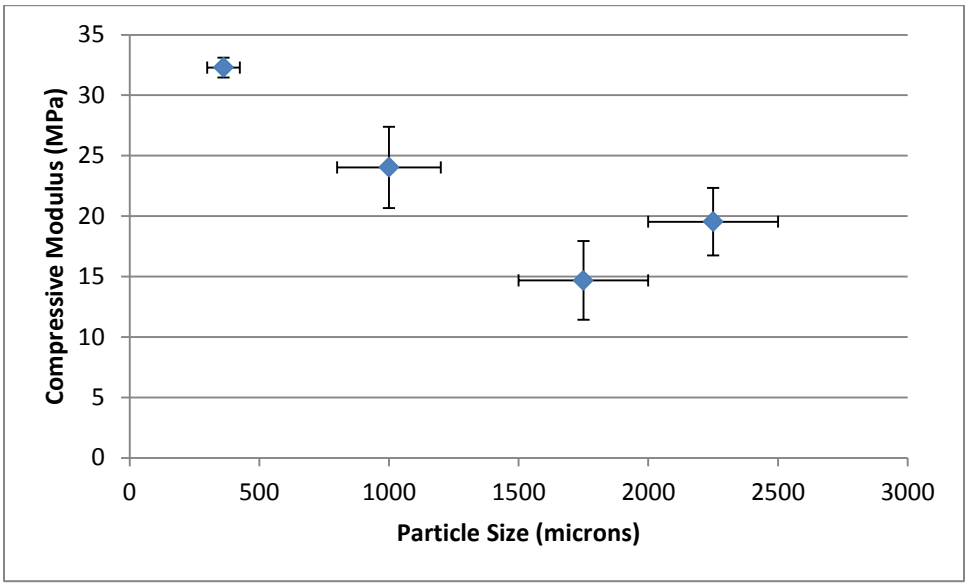

Figure 14 – Plot of glass bead size versus modulus at maximum vacuum pressure (100 kPa).

3.2 Other Materials

From microscope pictures, the particle sizes of the medium-fine glass blasting media were confirmed to be within the 88-149 µm range. From a sample of 20 grains, the measured size was 110 ± 23 µm. Oblong and deformed particles were also present en masse. Play sand and coffee particle sizes were determined to be on the order of 200-1000 and 100-1000 microns respectively. Sand and coffee grains both had considerably variable morphologies (Figure 15).

From the compression tests for coffee, sand, and blasting media, both yield stress and Young's modulus exhibited linear behavior with vacuum pressure (Figure 16 and 17). Coffee and sand both outperformed glass beads in yield stress and strength to weight ratio (Figure 18 and Table 3) and underperformed in effective Young's modulus.

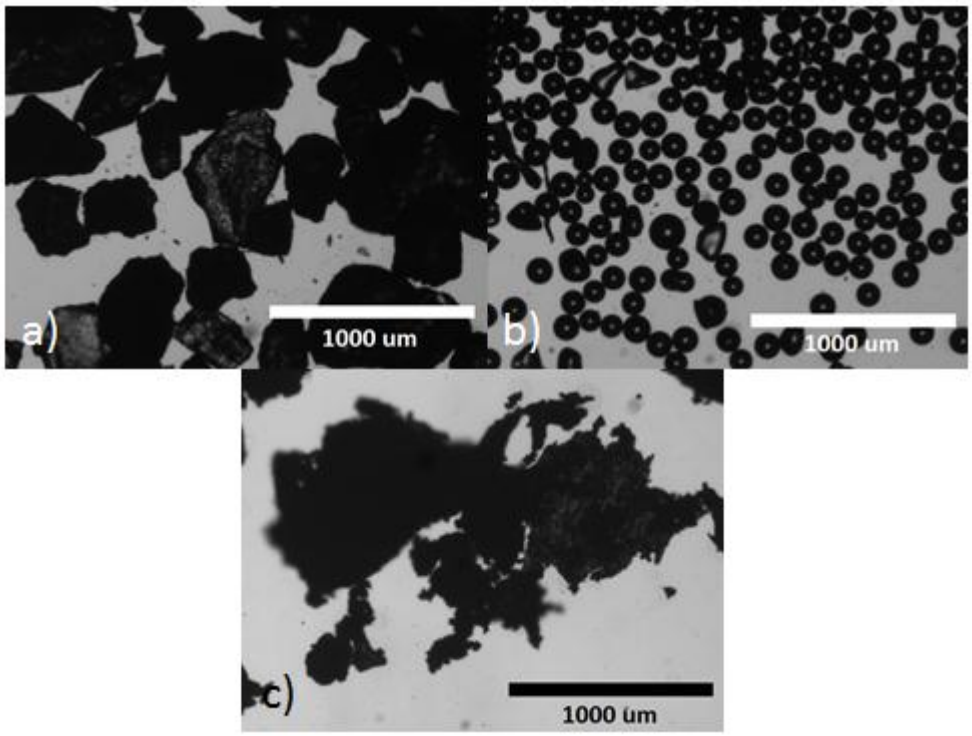

Figure 15 – Microscope pictures of a) play sand; b) medium-fine glass blasting media; c) ground coffee

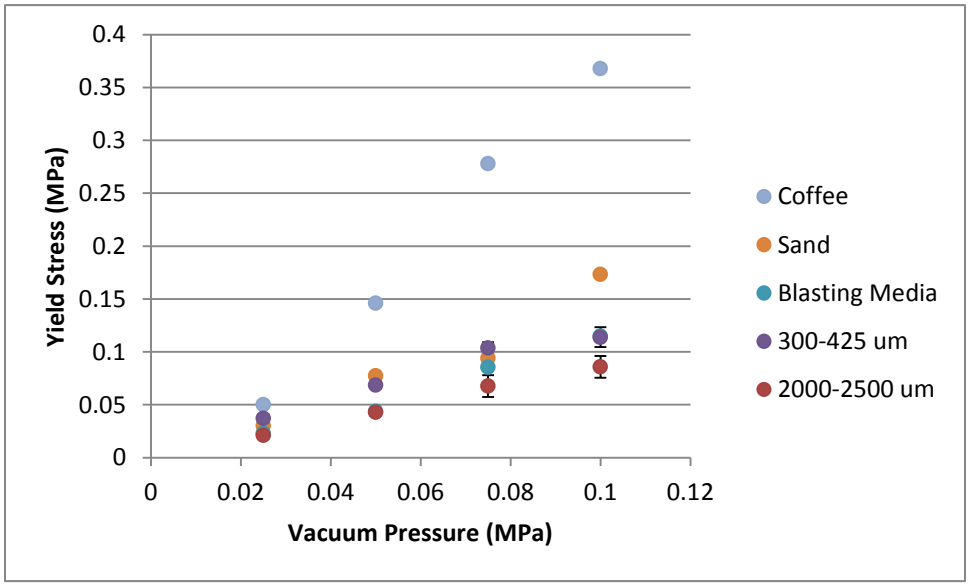

Figure 16 – Plot of yield stress with respect with vacuum pressure for sand, blasting media, and coffee. Extreme glass bead size values are included for comparison.

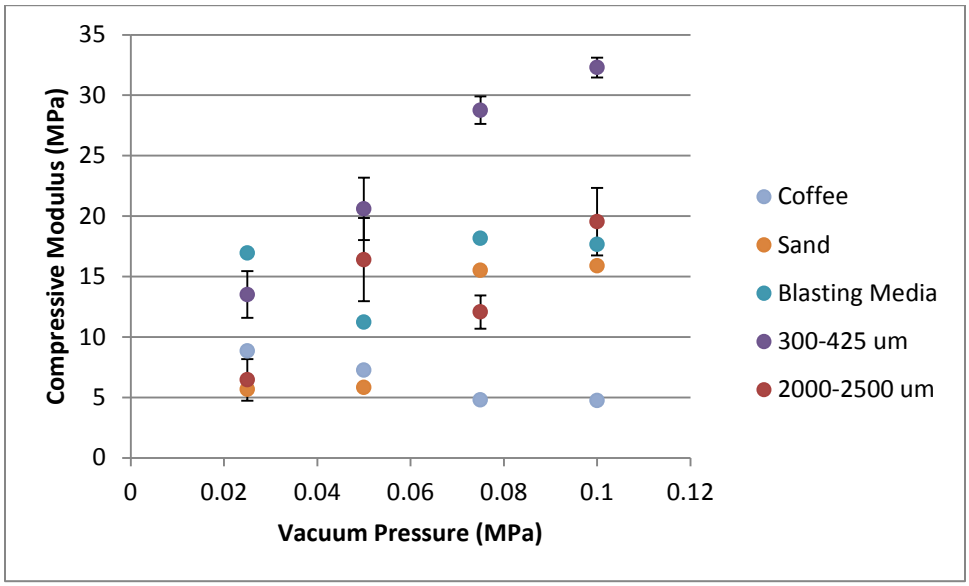

Figure 17 – Plot of Young's modulus with respect with vacuum pressure for sand, blasting media, and coffee. Extreme glass bead size values are included for comparison.

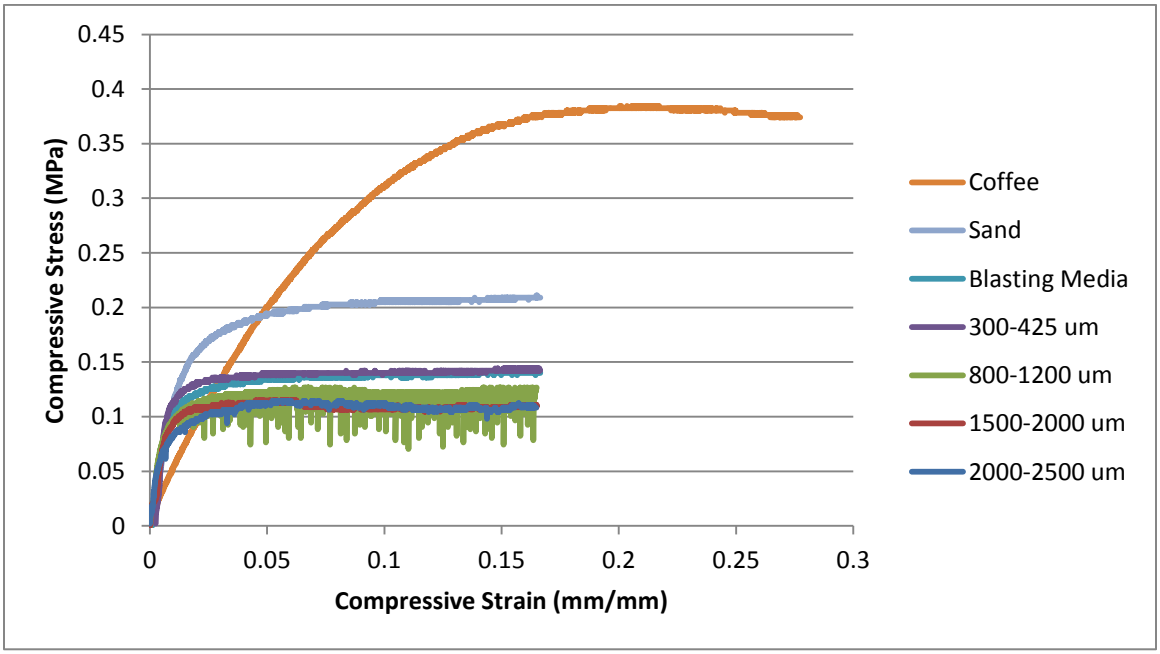

Figure 18 – Stress-strain curves of all materials under full vacuum (100 kPa).

Material	Yield Strength/Mass (10^{-4} MPa/g)
300-425 µm Silica Beads	4.1
800-1200 µm Silica Beads	3.8
1500-2000 µm Silica Beads	3.6
2000-2500 µm Silica Beads	3.1
Medium-Fine Silica Blasting Media (149-88 µm)	4.2
Play Sand	6.2
Ground Coffee	47.4

Table 3 – Strength to weight ratios of all materials at full vacuum.

Chapter 4: Discussion

4.1 Glass Beads

The major sources of error included the variability of the loose packed granular structure between each sample and the accuracy of the pressure gauge. During operation, the dial fluctuated within 1 MPa of the set value.

For maximum vacuum (100 kPa), the trends in modulus and yield strength with particle size appear to agree with theoretical predictions. As the cylindrical test sample deforms, the core of the sample will have a different mechanical behavior than the exterior. This is due to the change in the number of contacts between grains from the center to the outermost particles. As determined theoretically by Nagel, et al, yield behavior varies with coordination number. As seen in figure 19, the force distribution due to the number of contacts will create different yield criteria depending on location in the sample. The observed stress-strain curve is a combination of the properties of the bulk and exterior "curves".

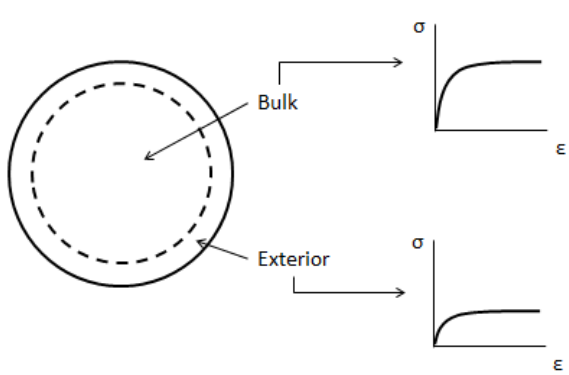

Figure 19 – Cross-section of sample undergoing deformation. Due to the difference in contact number, the bulk and exterior will have different mechanical properties.

As particle size decreases, the size of the exterior shell will decrease until it becomes negligible. As seen in Figures 11 and 12, yield stress as well as Young's modulus tends to increase with smaller particle size. In principle, for the given sample volume, the net coordination number of particles should decrease with size. The geometrical constrains do not allow the largest spheres to fully pack upon pouring. With a smaller particle size, constraints become less of an issue. Hence, the Young's modulus, as calculated by Somfai, et. al., should exhibit some power law behavior in principle. However, a power law relationship cannot be easily determined from these experiments. In theoretical simulations, the behavior has only been calculated for an ensemble of perfect spheres with uniform size, not of different size distributions. To determine whether or not there is a power law relationship for spheres with a distribution of sizes, more compression tests and simulations must be undertaken.

4.2 Other Materials

The mechanical performance of the sand and blasting media can be mostly attributed to the small particle size. Although the thickness of exterior layer particles decreased, the stress-strain curve of the blasting media is similar to that of 300-425 μm glass beads. Even with the amount of non-spherical particles to inhibit the degrees of freedom for the spheres to move would, in principle, create stronger bulk behavior. This phenomenon may hint at a yield strength limit with respect to particle size. It is

also possible that the amount of non-spherical grains decreased the bulk contact number which, analogous to network modifiers in a glass, would limit the distribution of internal stresses and cause the bulk to yield earlier. Nonetheless, more experimental and simulation data would have to be collected to resolve this question.

For play sand, the particles are hard and jagged. Such morphology would increase the contact area, upon an applied vacuum, increase friction between particles and limit the degrees of freedom of each grain. Hence, the sand has a higher yield stress than of all the other silica based materials.

Unlike the other materials, the coffee had particles that were deformable and jagged – very similar to some soils. The shapes of the coffee grains allow for friction, higher contact area, and lower degrees of freedom (all of which can increase strength). The ability for the grains to deform is another source of strength. Upon compression, the coffee grains first deform and densify before sliding. Additionally, capillary action is present from residual oils in the coffee. Due to its low density, coffee offers the highest strength to weight ratio than that of the other materials tested (Table 3).

Chapter 5: Conclusions

5.1 Conclusions

The glass spheres experiment verifies the computer prediction that applied pressures leads to an increase in Young's modulus. However, more data must be collected on spheres of the same size and packing fraction to verify the predicted power law relationship.

From compression tests, both sand and coffee offer the highest yield strength, which make them the most favorable material for mechanical applications such as joints, robotic manipulators, or jammable furniture. They offer a higher interparticle friction coefficient due to morphology and can easily flow without vacuum due to the large distribution of sizes. For specific applications, other procedures such as deflection and three point bending tests must be conducted to determine the optimal geometry (i.e cylinder dimensions) of the granular ensemble.

For applications such as low temperature casting, where high resolution is more critical and mechanical properties are not as much of an issue, materials like silica blasting media would be the best choice.

5.2 Future Work and Applications

Although ground coffee was found to have the highest yield strength, it has yet to be determined whether other types of ground coffee offer better results. The morphologies, size distribution, and amount of residual oils in the coffee likely vary between brands. Therefore more mechanical tests must be done to compare different types of coffee.

The use of heterogeneous granular media where the different components provide specific properties for the jammed system has yet to be significantly explored theoretically and experimentally. Rather than using a homogenous medium like sand or glass beads, specific properties could be enhanced by combining different media as in a traditional composite like glass fibers embedded in resin.

Composite grains could be of different shapes and materials to attain a desired stress-strain response of the system. One example is combining sand and metal jacks. Sand would provide compliance and flow in the unjammed state and compressive strength in the jammed state. Sand by itself would offer little tensile strength since particles can slide across one another. In tension there is no strength except the vacuum pressure acting on the system. By introducing jacks, the composite jammed system gains strength in tension and in bending from entanglement.

Composites could also be designed to provide volumetric effects, such as using foams to create larger volume changes and restoring forces when jamming. Optical and magnetic properties could also be tuned through composite jammed structures to provide feedback of the system's state, induce jamming pressure, or act as a sensor affected by external stimulus.

References

[1] Torquato, S; Stillinger, F.H. Multiplicity of generation, selection and classification procedures for jammed hard-particle packings. *J. Phys. Chem. B*. **105**: 11849-11853 (2001).

[2] Liu, A.; Nagel, S. The jamming transition and the marginally jammed solid. *Annu. Rev. Condens. Matter Phys*. **1**: 347-369 (2010).

[3] Lu, K.; Brodsky, E.; Kavehpour, H. A thermodynamic unification of jamming. *Nature Physics*, **4**: 404-407 (2008).

[4] Shokef, Y.; Liu, A. Jamming mechanisms and density dependence in a kinetically-constrained model. *Europhys. Lett.* **90**: 26005 (Apr. 2010).

[5]Corwin, E.I.; Jaeger, H.M.; Nagel, S.R. Structural signature of jamming in granular media. *Nature.* **435**: 1075-1078 (2005).

[6] Ludewig, F.; Vandewalle, N.; Dorbolo, S. Compaction of granular mixtures. *Granular Matter*, **8**(2): 87-91 (2006).

[7] Somfai, E.; vanHecke, M.; Ellenbroek, W.G.; Shyndyak, K.; vanSaarloos, W. Critical and noncritical jamming of frictional grains. *Phys. Rev. E.* **75**(2): 20301-1-4, (2007).

[8] Durian, D.J. Foam mechanics at the bubble scale. *Phys. Rev, E*. **75**(26): 4780-3, (2007).

[9] Brown, E.; Rodenberg, N.; Amend, J.; Mozeika, A.; Steltz, E.; Zakin, M.R.; Lipson, H.; Jaeger, H.M. Universal robotic gripper based on the jamming of granular material. *PNAS*, **107**(44): 18809-14, (2010).

[10] Mitsuda, T.; Kuge, S.; Wakabayashi, M.; Kawamura, S. Wearable. Haptic display by the use of a particle mechanical constraint. *2002 IEEE 10th Symp. on Haptic Interfaces for Virtual Envir. & Teleoperator Systs,* (2002).

[11] Annan, M.; Steltz, E.; Jaeger, H.M. The first steps of a robot based on jamming skin enabled locomotion. *IEEE/RSJ Int. Conf. Intelligent Rob. Syst., IROS* 2009, 408-409.

[12] Steltz, E.; Mozeika, A.; Rembisz, J.; Corson, N.; Jaeger, H.M. Jamming as an enabling technology for soft robotics. *2010 SPIE Conf. on Electroactive Polymer Actuators and Devices*, **7642**, (2010).

[13] Wu, Y.; Casanova, H.; Smith, W. CIR casting system: a new approach for making transtibial sockets. *IDEAnet Technical Brief*, March 2004

[14] Keating, S; Hudson, S.; Oxman, N.; Cheng, N.; Lieven, O.; Gero, K.; Hosoi, A. Design using jammable granular systems. *Northeastern Granular Materials Workshop*, June 2011.

[15] Germaine, J.; Germaine, A. *Geotechnical Laboratory Measurements for Engineers.* John Wiley & Sons: Hoboken, NJ. (2009).

Appendices

A. Young's Modulus Calculation Algorithm

The Instron Bluehill testing software allows for automatic calculation of Young's modulus from the raw data. The system begins by searching the data for the first data point to the maximum load value and carries out a zero-slope yield calculation to determine if a yield point exists in the data series. Using the first data point as the start value and the yield point or maximum load point (whichever comes first), the system divides the data on the stress axis between the start and end values in six equal regions with 0% overlap. Then a least squares fit algorithm is applied to all the points in the each region to determine the slope of each region. After the slope calculation, the system determines the pair of consecutive regions that has the highest slope sum. From this pair, the region with the highest slope is determined and is assigned the modulus value.

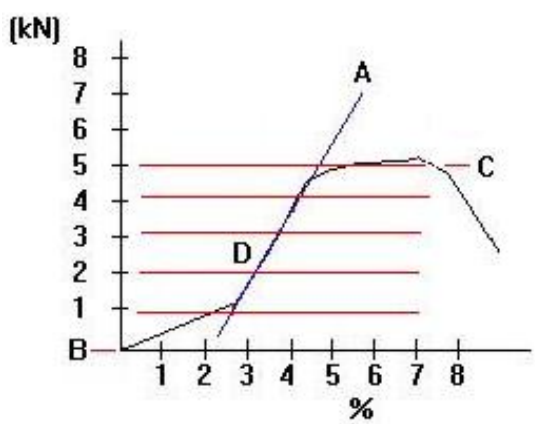

Figure 20 – Example load-displacement curve demonstrating the Young's modulus calculation algorithm using a least squares fit.

In the example shown in Figure 20, the first data point, B, is the start value at 0 kN and C is the end value of 5 kN. The data between these points is divided evenly into six regions. The third region was found to have the greatest slope and therefore the system constructs a modulus line along the slope of that region.

B. Yield Stress Calculation Algorithm

This calculation determines the point on the stress-strain curve at which yield is assumed to have taken place. Slope threshold yield is a depended calculation that requires a result from the modulus calculation. The slope threshold yield calculation searches for the point at which the slope of the stress-strain curve has decreased to a specified percentage of the modulus slope.

The system first divides the curve into 100 regions with 0% overlap, calculates the slope of each region, then finds the first region with a slope less than or equal to 10% of the specified modulus slope. The yield point is assigned to the center point of this region.

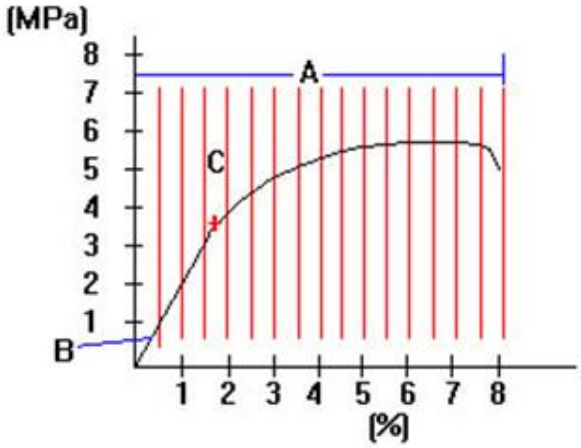

Figure 21 - Example load-displacement curve demonstrating the yield stress calculation algorithm using the modulus slope threshold criterion.

In the example shown in Figure 21, the stress-strain curve is divided into A regions. The first region, B, contains the initial slope. The data in the fourth region, C,

is the first point at which the slope drops 10% of the initial slope. The yield stress is assigned at the center of the region.

C. Stress-Strain Curves

C.1 300-425 um Glass Beads:

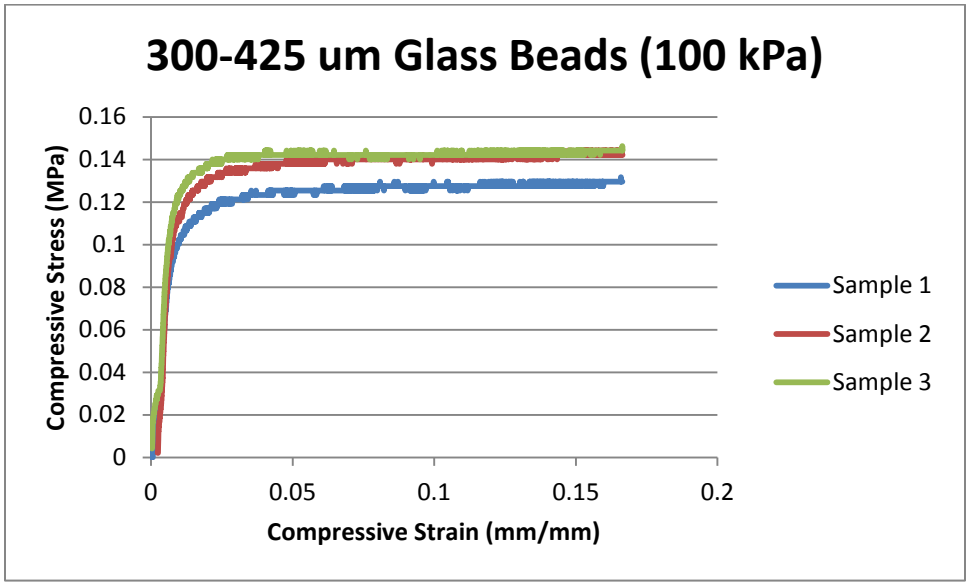

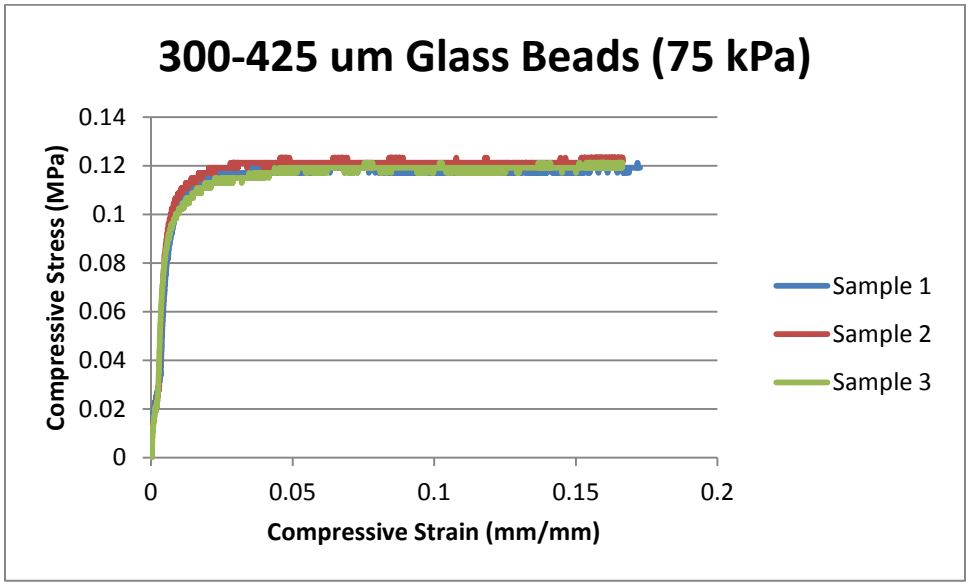

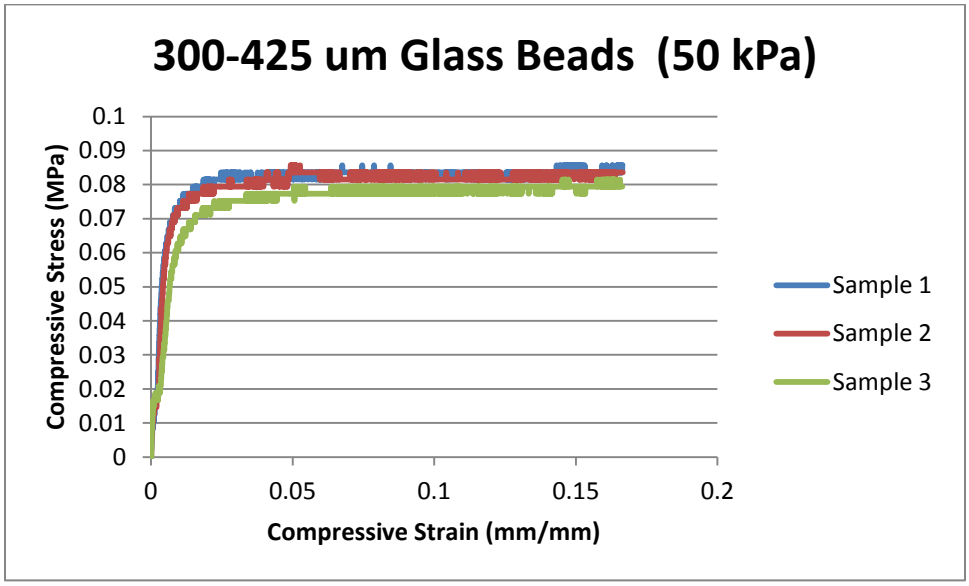
300-425 um Glass Beads (50 kPa)
Compressive Stress (MPa)
0.1
0.09
0.08
0.07
0.06
0.05
0.04
0.03
0.02
0.01
0
0
0.05
0.1
0.15
0.2
Compressive Strain (mm/mm)
Sample 1
Sample 2
Sample 3

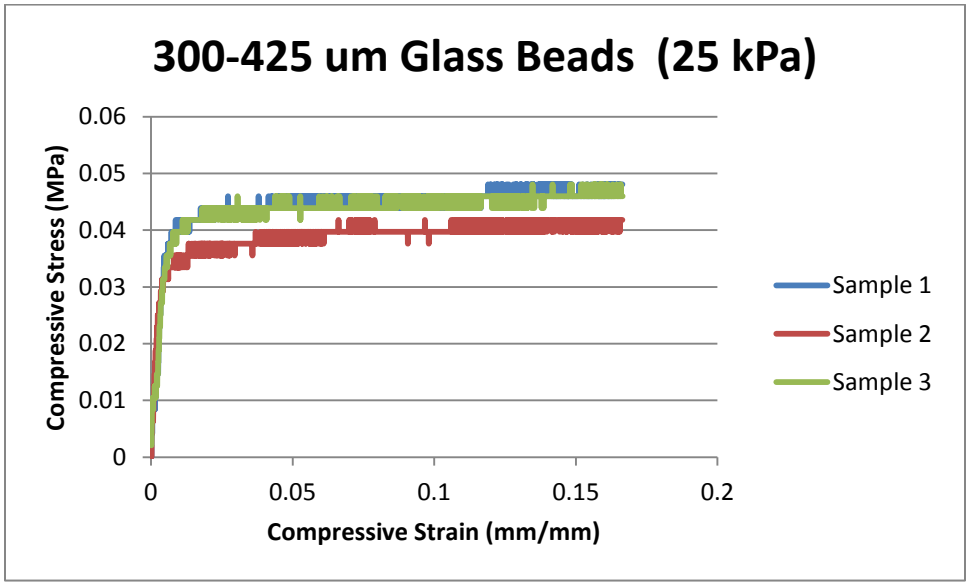
300-425 um Glass Beads (25 kPa)
Compressive Stress (MPa)
0.06
0.05
0.04
0.03
0.02
0.01
0
0
0.05
0.1
0.15
0.2
Compressive Strain (mm/mm)
Sample 1
Sample 2
Sample 3

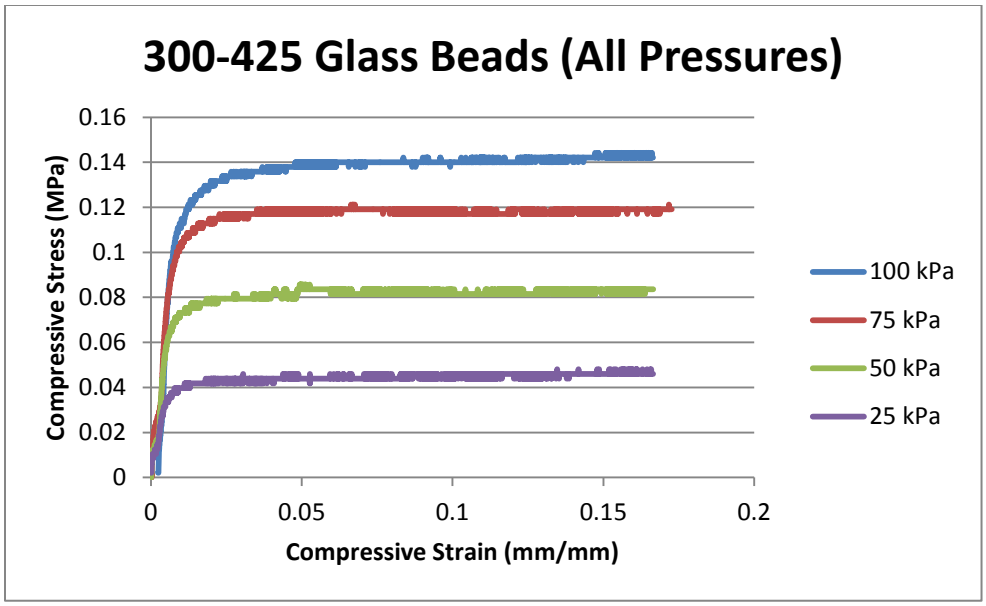

C.2 800-1200 um Glass Beads:

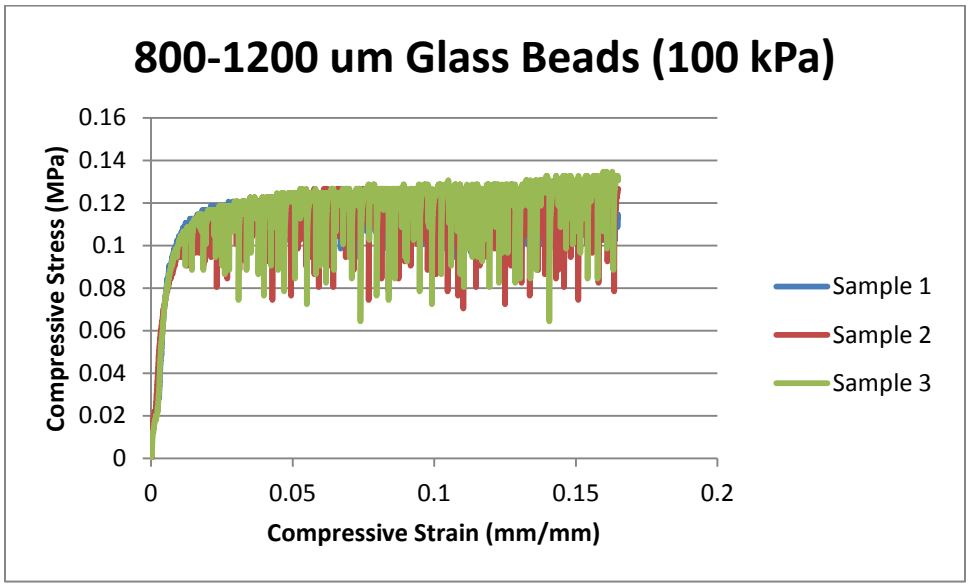

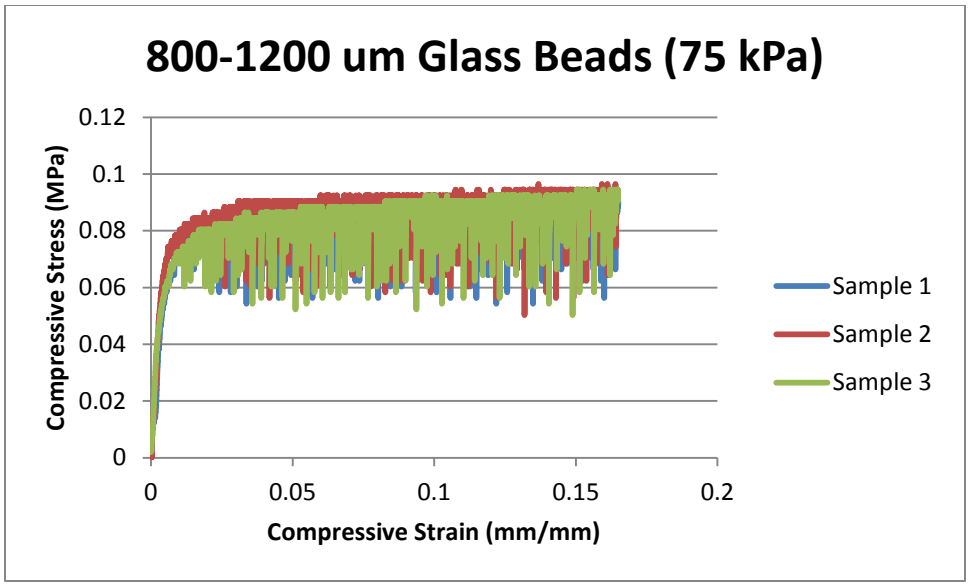
800-1200 um Glass Beads (75 kPa)
Compressive Stress (MPa)
0.12
0.1
0.08
0.06
0.04
0.02
0
0
0.05
0.1
0.15
0.2
Compressive Strain (mm/mm)
Sample 1
Sample 2
Sample 3

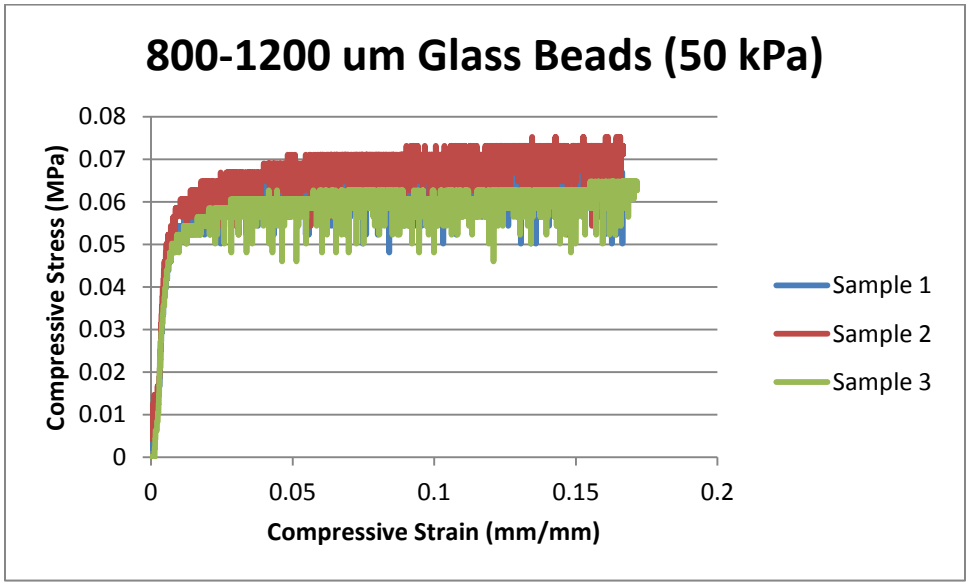
800-1200 um Glass Beads (50 kPa)
Compressive Stress (MPa)
0.08
0.07
0.06
0.05
0.04
0.03
0.02
0.01
0
0
0.05
0.1
0.15
0.2
Compressive Strain (mm/mm)
Sample 1
Sample 2
Sample 3

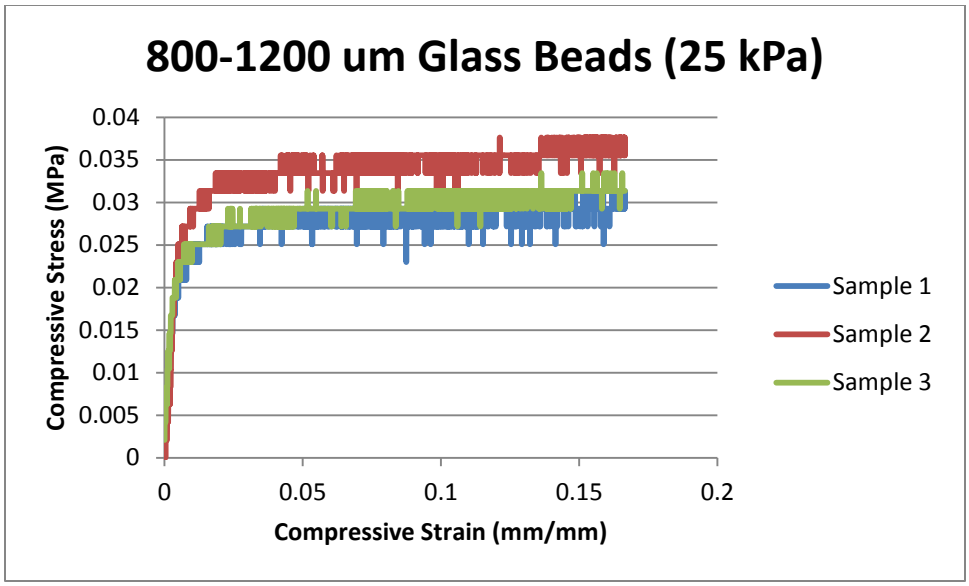
800-1200 um Glass Beads (25 kPa)
Compressive Stress (MPa)
0.04
0.035
0.03
0.025
0.02
0.015
0.01
0.005
0
0
0.05
0.1
0.15
0.2
Compressive Strain (mm/mm)
Sample 1
Sample 2
Sample 3

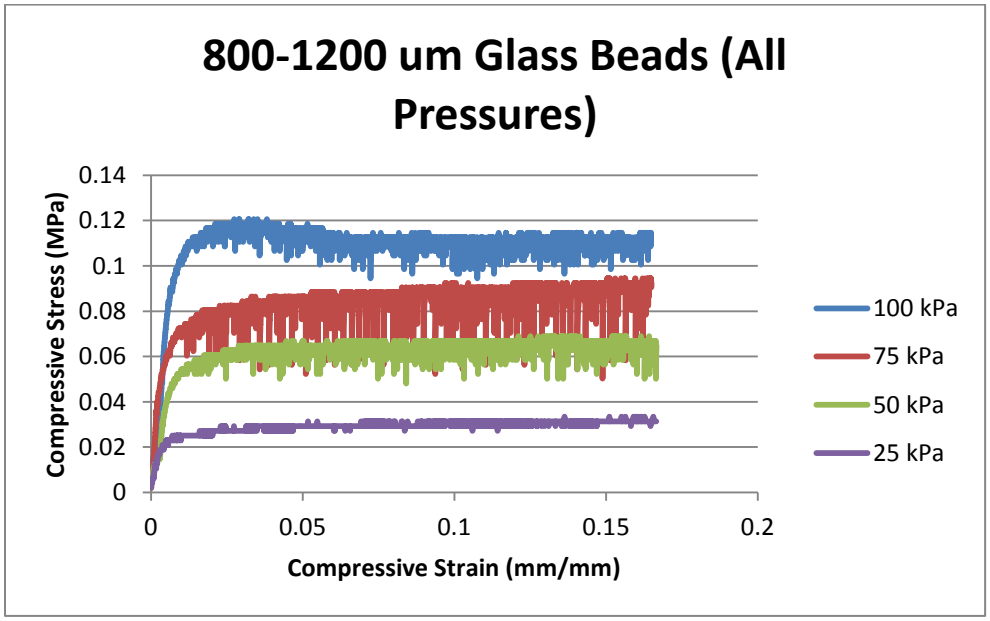
800-1200 um Glass Beads (All Pressures)
Compressive Stress (MPa)
0.14
0.12
0.1
0.08
0.06
0.04
0.02
0
0
0.05
0.1
0.15
0.2
Compressive Strain (mm/mm)
100 kPa
75 kPa
50 kPa
25 kPa

C.3 1500-2000 um Glass Beads

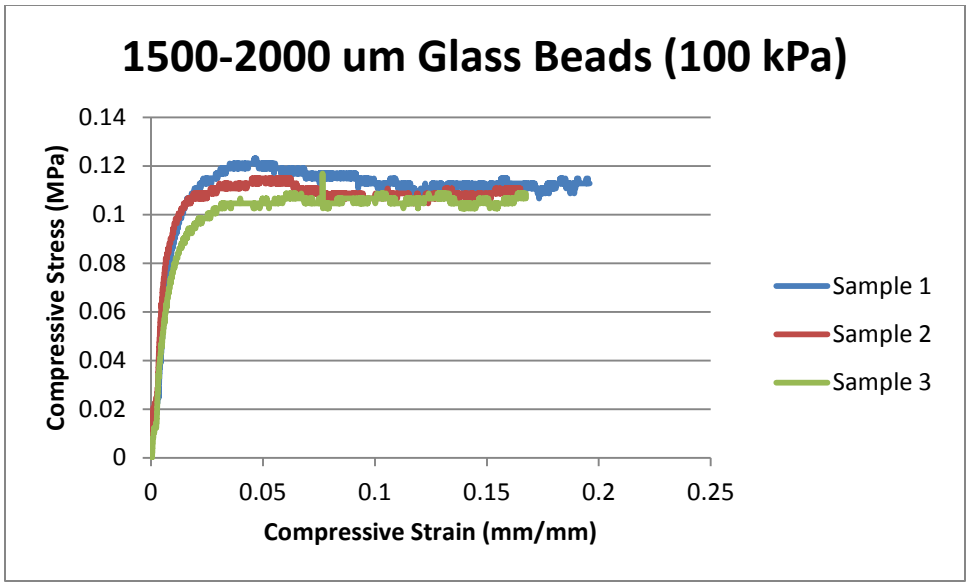

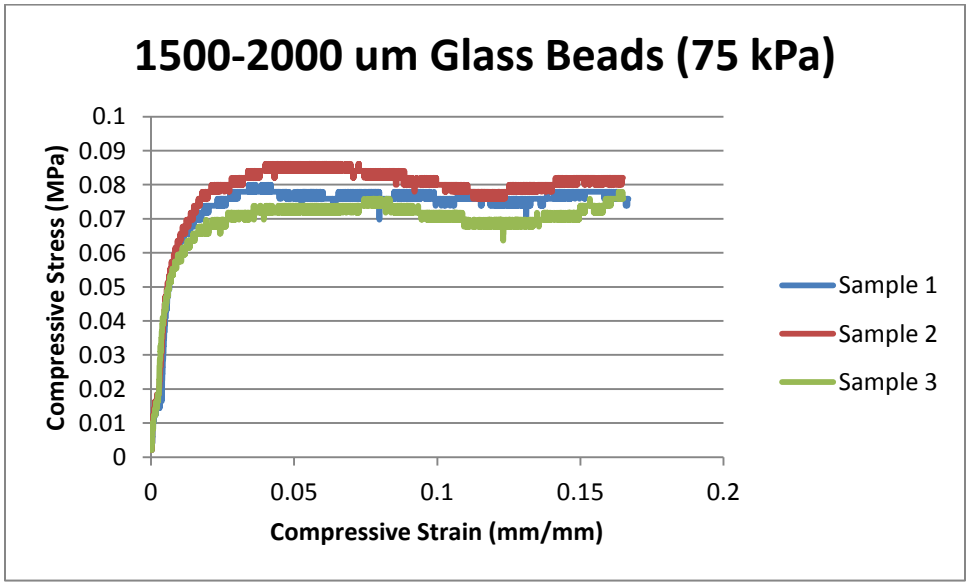

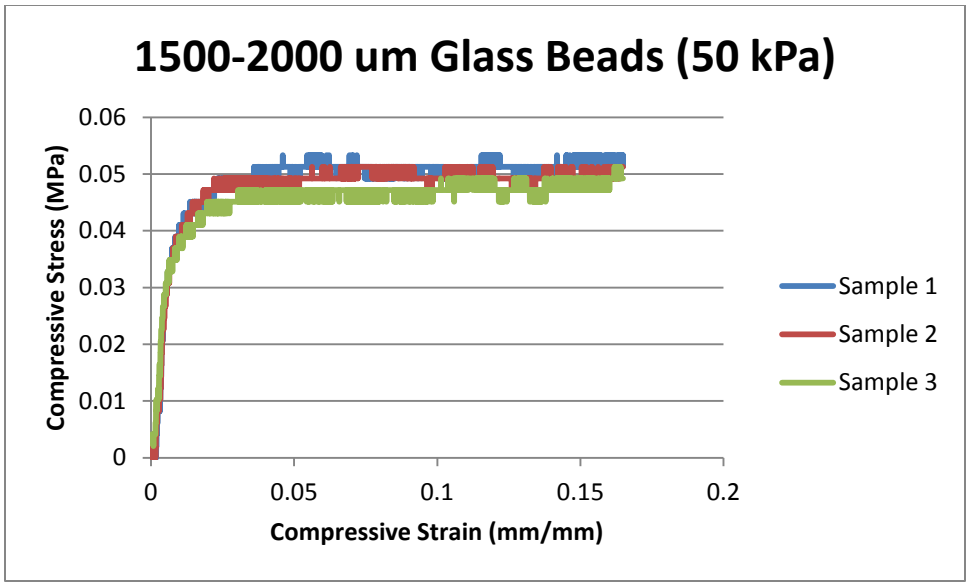
1500-2000 um Glass Beads (50 kPa)
Compressive Stress (MPa)
0.06
0.05
0.04
0.03
0.02
0.01
0
0
0.05
0.1
0.15
0.2
Compressive Strain (mm/mm)
Sample 1
Sample 2
Sample 3

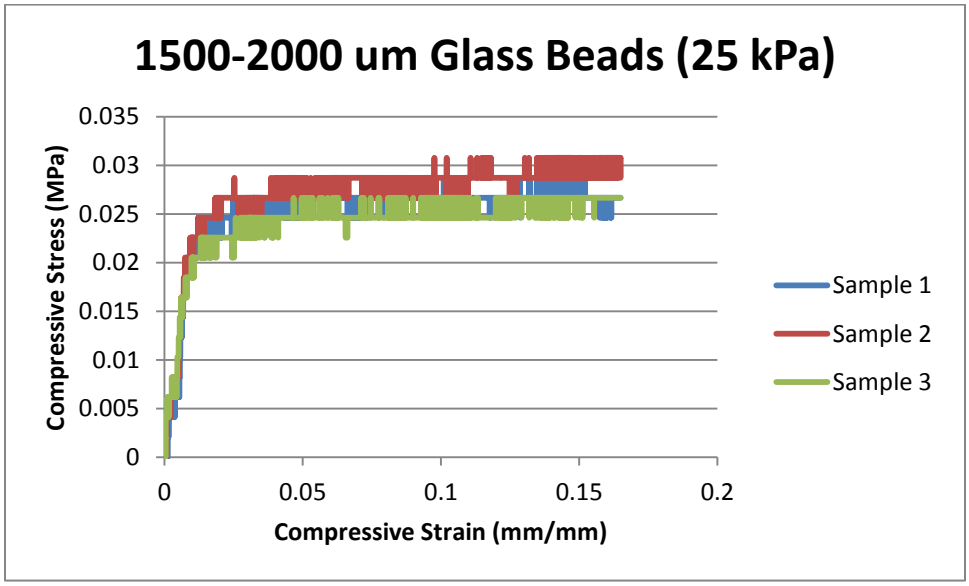
1500-2000 um Glass Beads (25 kPa)
Compressive Stress (MPa)
0.035
0.03
0.025
0.02
0.015
0.01
0.005
0
0
0.05
0.1
0.15
0.2
Compressive Strain (mm/mm)
Sample 1
Sample 2
Sample 3

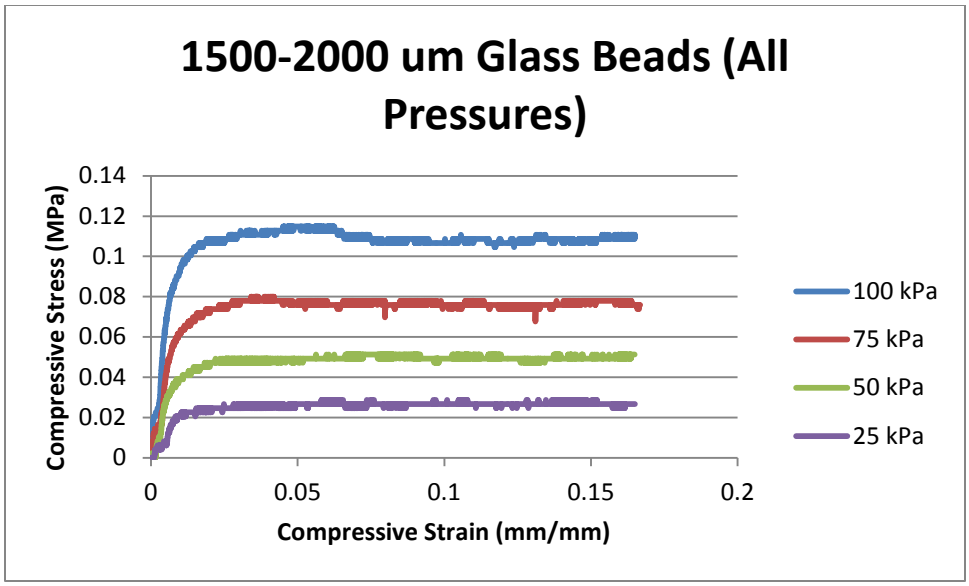

C.4 2000-2500 um Glass Beads

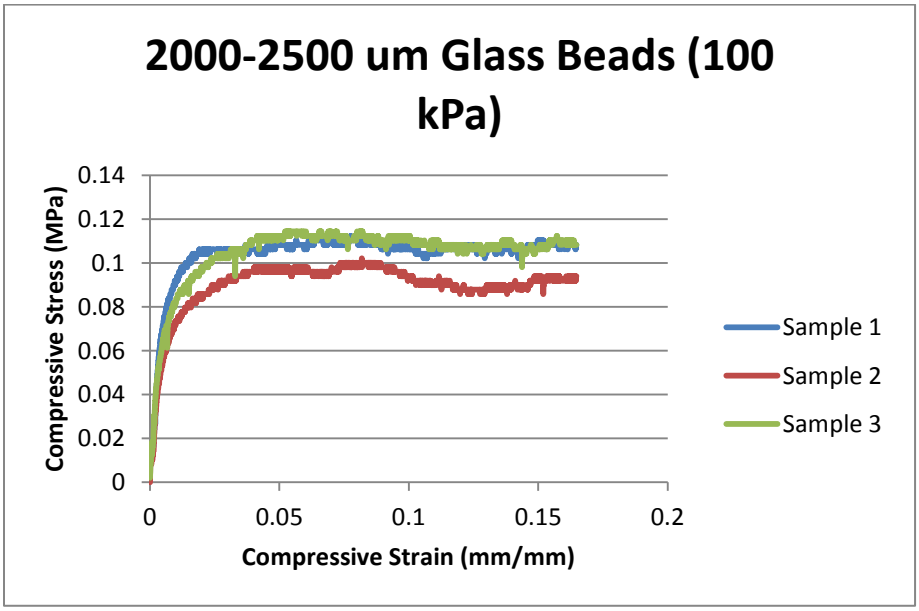

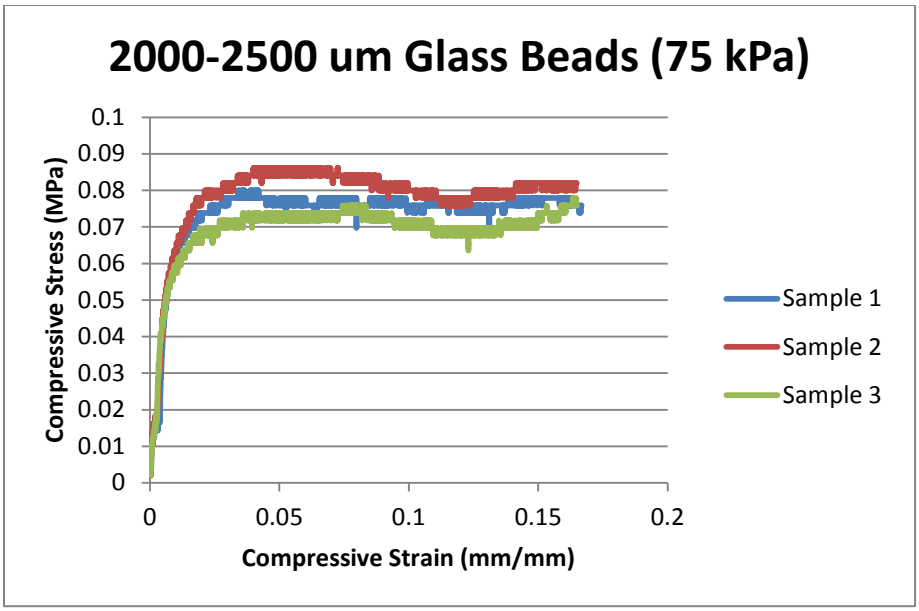
2000-2500 um Glass Beads (75 kPa)
Compressive Stress (MPa)
0.1
0.09
0.08
0.07
0.06
0.05
0.04
0.03
0.02
0.01
0
0
0.05
0.1
0.15
0.2
Compressive Strain (mm/mm)
Sample 1
Sample 2
Sample 3

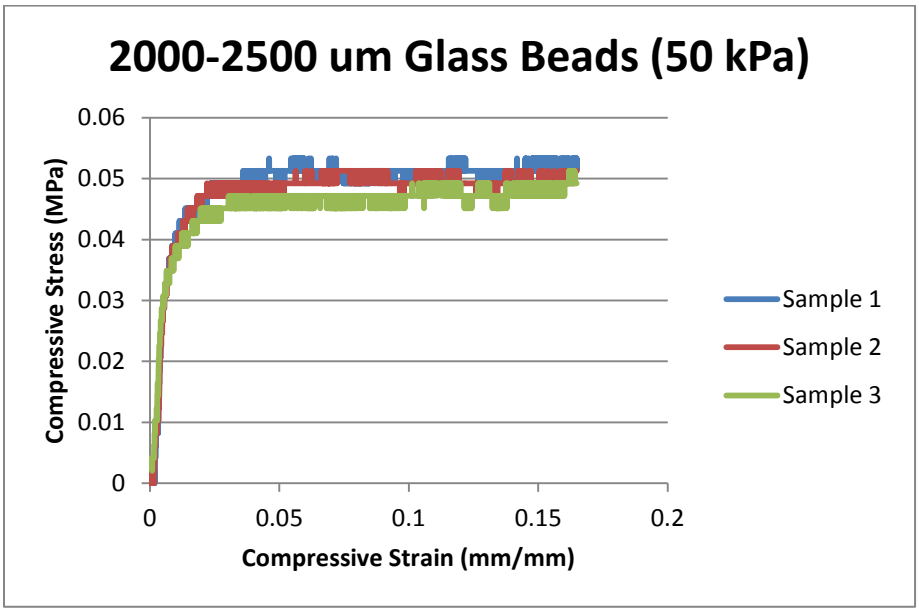
2000-2500 um Glass Beads (50 kPa)
Compressive Stress (MPa)
0.06
0.05
0.04
0.03
0.02
0.01
0
0
0.05
0.1
0.15
0.2
Compressive Strain (mm/mm)
Sample 1
Sample 2
Sample 3

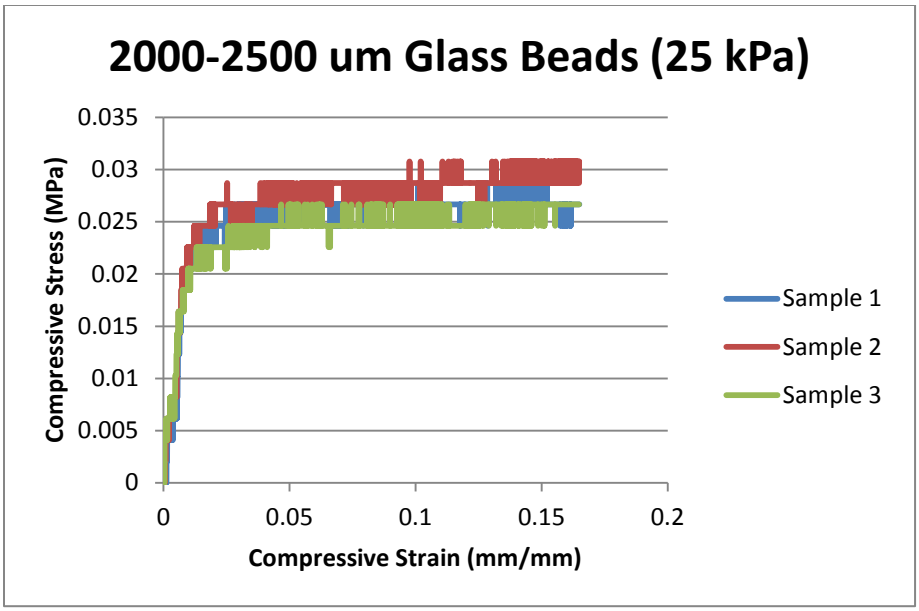
2000-2500 um Glass Beads (25 kPa)
Compressive Stress (MPa)
0.035
0.03
0.025
0.02
0.015
0.01
0.005
0
0
0.05
0.1
0.15
0.2
Compressive Strain (mm/mm)
Sample 1
Sample 2
Sample 3

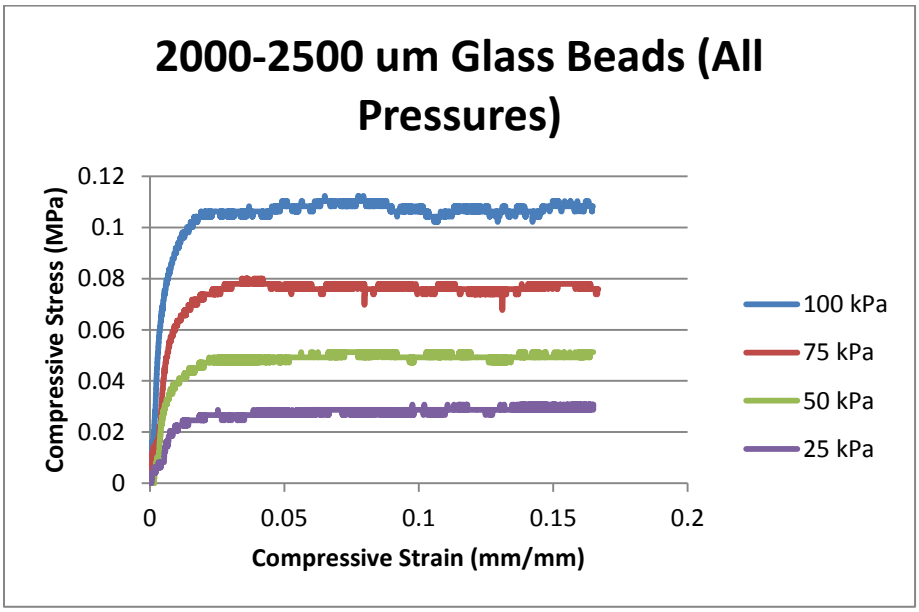
2000-2500 um Glass Beads (All Pressures)
Compressive Stress (MPa)
0.12
0.1
0.08
0.06
0.04
0.02
0
0
0.05
0.1
0.15
0.2
Compressive Strain (mm/mm)
100 kPa
75 kPa
50 kPa
25 kPa

C.5 Medium-Fine Glass Blasting Media

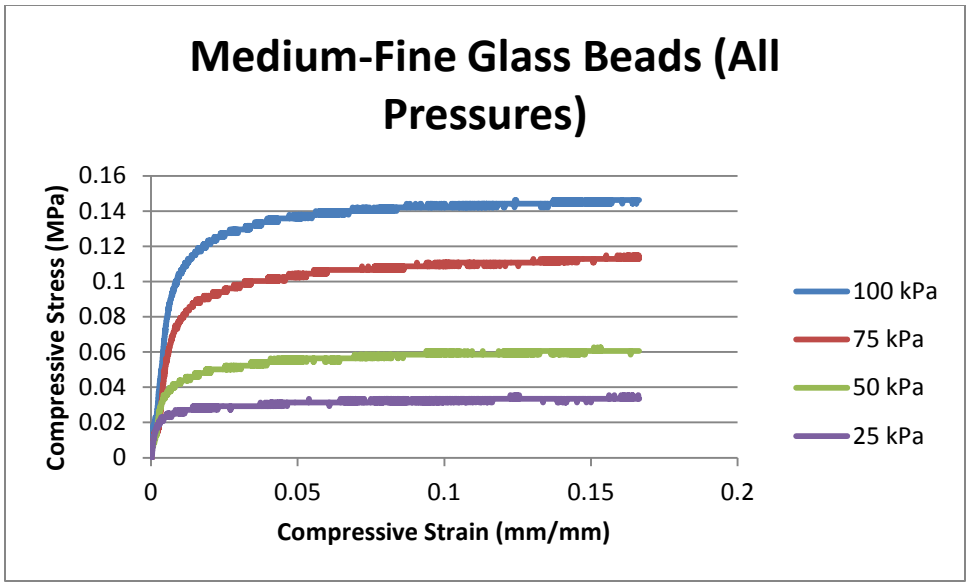

C.6 Ground Coffee

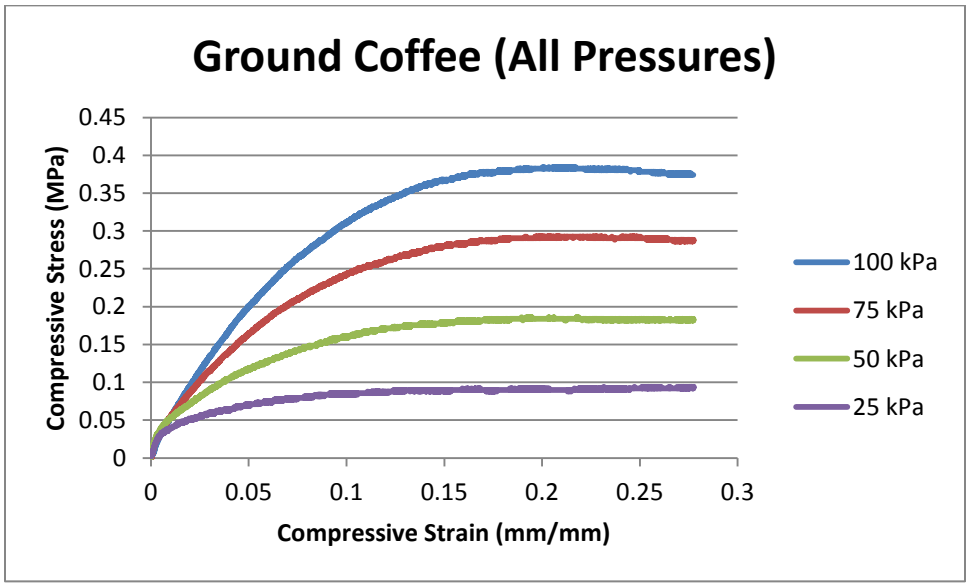

C.7 Play Sand

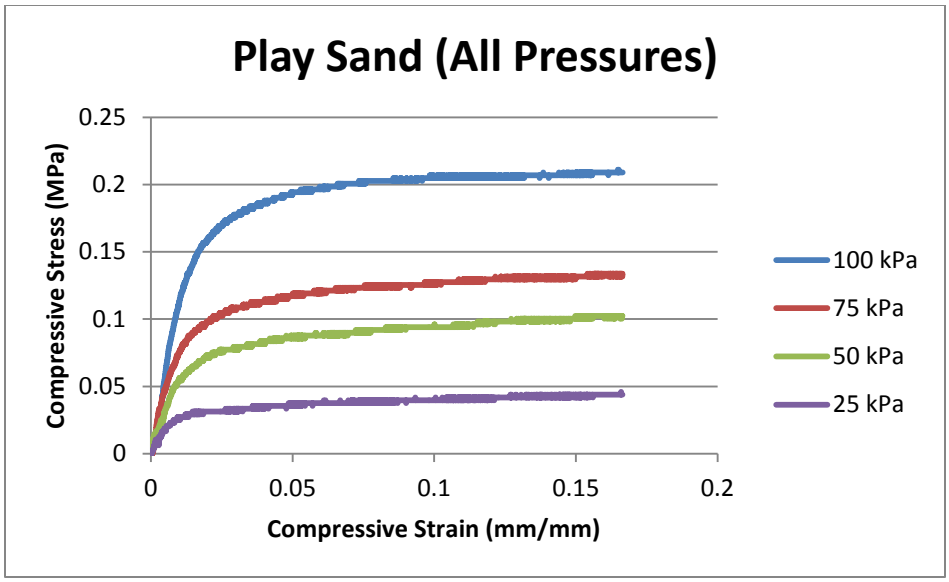
Play Sand (All Pressures)
Compressive Stress (MPa)
0.25
0.2
0.15
0.1
0.05
0
0
0.05
0.1
0.15
0.2
Compressive Strain (mm/mm)
100 kPa
75 kPa
50 kPa
25 kPa